Supplementary Informations

pH-Responsive Intelligent Anticorrosion Protection: Catechol-Driven Organic-Inorganic Hybridization with TiO_2 and Encapsulation by ZIF-90

Jianfeng Hu[a]* Huiya Cheng[a]

(a School of Chemistry and Chemical Engineering, South China University of Technology, Guangzhou 510640, China)

*Corresponding author.

E-mail: cejfhu@scut.edu.cn (J. Hu).

Methods

1. Fourier transform infrared spectroscopy (FT-IR)

The chemical compositions of PVP, DH, PD, PDT, ZIF-90, and PDT@ZIF-90 were characterized by FTIR spectroscopy (Nicolet IS50, Thermo Scientific Continuum platform) using KBr pellet matrices, with spectral acquisition spanning the mid-infrared region (4000–400 cm^{-1}).

2. X-ray diffraction (XRD)

The structure of the samples was characterized by X-ray diffraction (XRD, Rigaku MiniFlex600, Japan) with a scanning range of 5–90° and a scanning rate of 10 °/min.

3. Thermal analysis (TGA)

The thermal stability and degradation behavior of PVP, DH, TiO_2, PD, PDT, ZIF-90, and PDT@ZIF-90 were investigated using a

thermogravimetric analyzer (TGA, 550). Measurements were performed under a nitrogen atmosphere, with samples heated from 35 °C to 600 °C at a constant heating rate of 10 °C/min. The mass loss of each sample was recorded as a function of temperature.

4. Morphological characterization (SEM, TEM)

The morphology and structure of TiO_2, PD, PDT, ZIF-90, and PDT@ZIF-90 were observed and characterized by scanning electron microscopy (SEM, SU8220). Transmission electron microscopy (TEM, Thermo Fisher Talos F200S) and coupled energy dispersive spectroscopy (EDS) were used for further structural and elemental analysis.

5. Characterization of Q235 surface morphology

The surface morphology of Q235 carbon steel samples was examined using a scanning electron microscope (SEM, Thermo Fisher Scientific Quanta FEG 250, USA) operated at an accelerating voltage of 10 kV. Prior to SEM observation, the blank sample (untreated Q235 steel) was mechanically polished with 2000-grit abrasive sandpaper, while all samples (including the blank) were cleaned in anhydrous ethanol three times and dried in an oven at 40 °C for 6 hours. To enhance conductivity, the samples were sputter-coated with a 5 nm gold layer using an ion sputter coater.

6. Corrosion analysis (XPS)

Corrosion products were analyzed by X-ray photoelectron spectroscopy (XPS, Thermo Fisher Scientific K-Alpha, USA) with Al Kα radiation (1486.68 eV). Spectra were calibrated by referencing the C 1s peak to 284.8 eV.

7. Quantum Chemical Calculations

Quantum chemical calculations were performed using density functional theory (DFT) with the B3LYP hybrid functional and 6-31G(d,p) basis

set implemented in Gaussian 09. The molecular geometries of polyvinylpyrrolidone (PVP), dopamine hydrochloride (DH), and the synthesized corrosion inhibitor PD were fully optimized at the B3LYP/6-31G(d,p) level. Frontier molecular orbital analysis was conducted to determine the energies of the highest occupied molecular orbital (HOMO), the lowest unoccupied molecular orbital (LUMO), and the resultant HOMO-LUMO energy gap (ΔE), which are critical for evaluating electron transfer properties

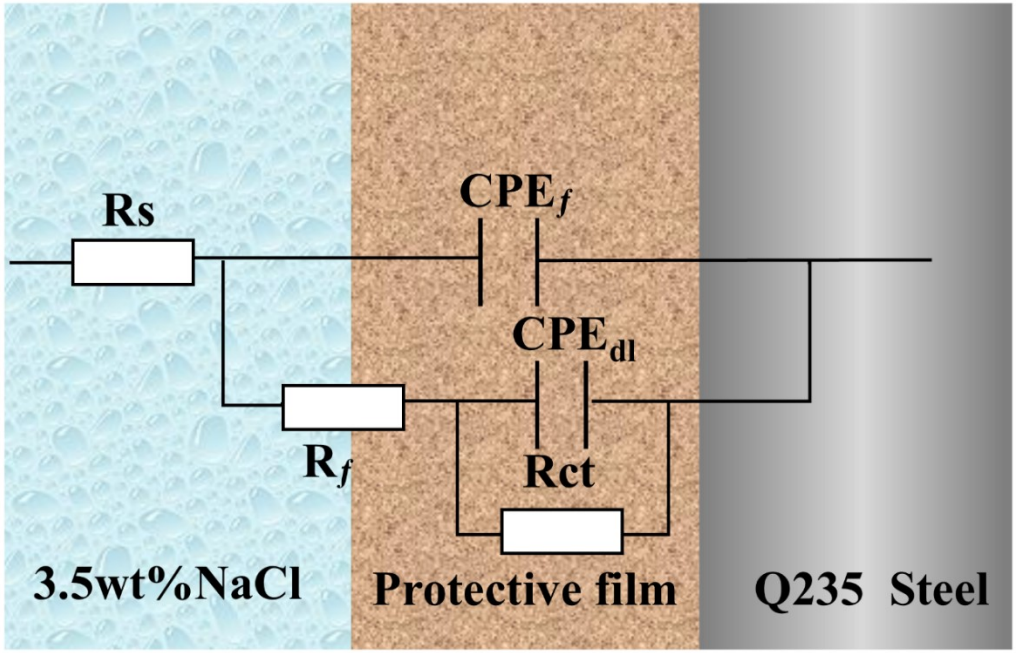

Fig. S1. Equivalent circuits used for EIS fitting.

Table S1 EIS parameters for the corrosion of Q235 in 3.5 wt.% NaCl at 298 K.

	Concentration(ppm)	$R_s(\Omega \cdot cm^2)$	Q_f		$R_f(\Omega \cdot cm^2)$	Q_{dl}		$R_{ct}(\Omega \cdot cm^2)$	$R_p(\Omega \cdot cm^2)$	η(%)
			Y_0 ($\Omega^{-1}s^n cm^{-2}$)	n_f		Y_0 ($\Omega^{-1}s^n cm^{-2}$)	n_{dl}			
blank	0	3.608	(9.407±)×10^{-8}	0.98	12.67	0.0031	0.72	146.9	159.57	-
	10	1.778	7.821E-006	0.662	4.11	0.00464	0.5864	270.3	274.41	41.8
	50	1.885	6.481E-006	0.6802	4.359	0.00413	0.6085	325.2	329.559	51.6
PVP	100	1.622	5.993E-006	0.7213	3.688	0.003822	0.6638	365.7	369.388	56.8
	150	0.867	5.881E-006	0.7401	4.394	0.003607	0.6746	402.2	406.594	60.8
	200	1.61	5.698E-006	0.7284	3.476	0.004273	0.7457	425.3	428.776	62.7
	10	2.019	3.96E-005	0.6621	5.246	0.004559	0.5956	301.0	306.246	43.9
	50	2.005	1.669E-005	0.7286	4.32	0.004321	0.656	353.9	358.22	52.4
DH	100	1.201	4.552E-005	0.5761	5.032	0.004719	0.6966	378.8	383.832	58.4

	150	1.0867	5.881E-006	0.7401	4.394	0.003607	0.6746	402.2	406.594	60.8
	200	1.383	5.878E-006	0.7506	4.596	0.005056	0.7007	436.2	440.801	63.8
	10	2.093	5.088E-006	0.7692	4.8	0.004262	0.6206	274.3	279.1	42.8
	50	1.879	5.331E-006	0.8444	4.567	0.003666	0.6605	303.9	308.467	48.3
TiO_2	100	2.407	5.706E-006	0.7678	5.019	0.003571	0.6994	338.7	343.719	53.6
	150	2.116	5.833E-006	0.8078	4.389	0.004013	0.7208	361.7	366.089	56.4
	200	2.305	6.72E-006	0.7248	4.662	0.00422	0.7728	376.4	381.062	58.1
	10	2.367	7.408E-007	0.8275	6.4	0.00374	0.4904	371.728	378.128	57.8
	50	1.451	5.508E-006	0.7591	6.503	0.003731	0.5965	431.876	438.379	63.6
PD	100	1.889	2.678E-006	0.8807	5.19	0.003144	0.6369	545.051	550.241	71.0
	150	2.088	3.903E-006	0.8229	5.504	0.002513	0.724	670.64	676.144	76.4
	200	2.377	2.357E-006	0.8346	6.233	0.003274	0.792	725.739	731.972	78.2
	10	2.004	5.785E-006	0.7795	5.216	0.002208	0.651	395.7	400.916	60.2
	50	2.201	5.064E-006	0.808	5.719	0.002311	0.7077	552.8	558.519	71.4
PDT	100	2.778	6.874E-006	0.7891	6.209	0.002681	0.7557	1091	1097.209	85.4
	150	2.142	5.824E-006	0.7873	5.445	0.002558	0.7889	1438	1443.445	88.9
	200	2.468	6.946E-006	0.7743	6.762	0.002054	0.8311	1801	1807.762	91.2

	10	2.281	6.314E-006	00.641 1	6.06	0.002347	0.7861	646.9	652.96	75.6
	50	3.777	7.011E-006	0.7638	6.876	0.002119	0.8113	1309	1315.876	87.9
PDT@ZIF-90	100	2.307	5.832E-006	0.7193	6.341	0.001873	0.8244	2333	2339.341	93.2
	150	2.313	6.641E-006	0.7305	6.327	0.001233	0.8298	3053	3059.327	94.8
	200	3.444	6.963E-006	0.7733	7.519	0.001002	0.8439	3313	3320.519	95.2
	10	1.573	5.024E-006	0.7563	2.386	0.004143	0.4432	224.971	228.930	30.3
	50	1.932	3.786E-005	0.7321	3.126	0.004559	0.4387	275.374	280.432	43.1
ZIF-90	100	2.036	5.241E-006	0.8025	2.976	0.004266	0.4923	306.041	311.053	48.7
	150	1.339	6.712E-006	0.7361	3.289	0.004013	0.4465	386.474	391.102	59.2
	200	1.763	5.675E-006	0.7335	3.112	0.004273	0.4532	407.445	412.320	61.3

Table S2 Polarization curve parameters for the corrosion of Q235 in 3.5 wt.% NaCl at 298 K

sample	Concentration/ppm	$-E_{corr}$/mV	i_{corr}/μA·cm^{-2}	η_{PDP}/%
blank	0	933	172.9	-
PVP	10	936	91.7	46.9

	50	923	85.68	50.4
	100	918	78.14	54.8
	150	951	67.97	60.7
	200	938	64.12	62.9
DH	10	977	87.26	49.5
	50	916	77	55.5
	100	991	74	58.4
	150	963	70.35	59.3
	200	927	61.03	64.7
TiO_2	10	914	102.4	40.8
	50	954	88.71	48.7
	100	948	82.62	52.2
	150	879	75.63	56.3
	200	908	72.33	58.2
PD	10	962	70.41	59.3
	50	976	67.41	61.0
	100	910	49.56	71.3

	150	888	42.32	75.5
	200	858	38.20	77.9
PDT	10	968	67.89	60.7
	50	980	49.94	71.1
	100	906	26.71	84.6
	150	876	19.49	88.7
	200	852	15.10	91.3
PDT@ZIF-90	10	976	42.18	75.6
	50	990	20.6	87.9
	100	944	11.2	93.5
	150	917	8.9	94.8
	200	892	8.3	95.2

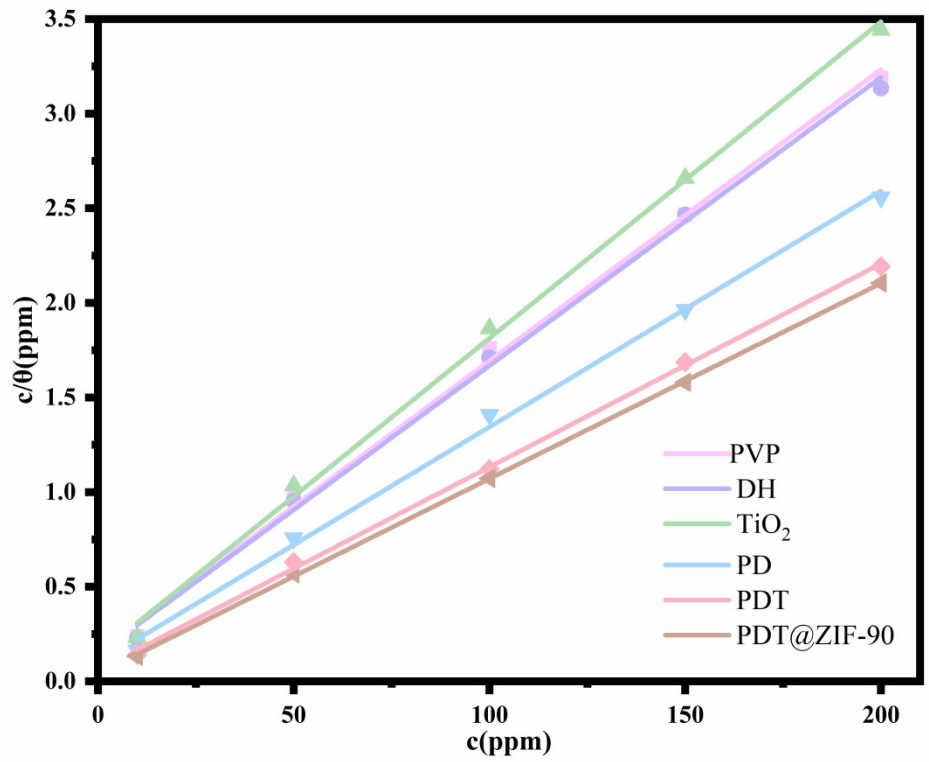

Fig.S2. Langmuir adsorption isothenm for the test inhibitors on Q235

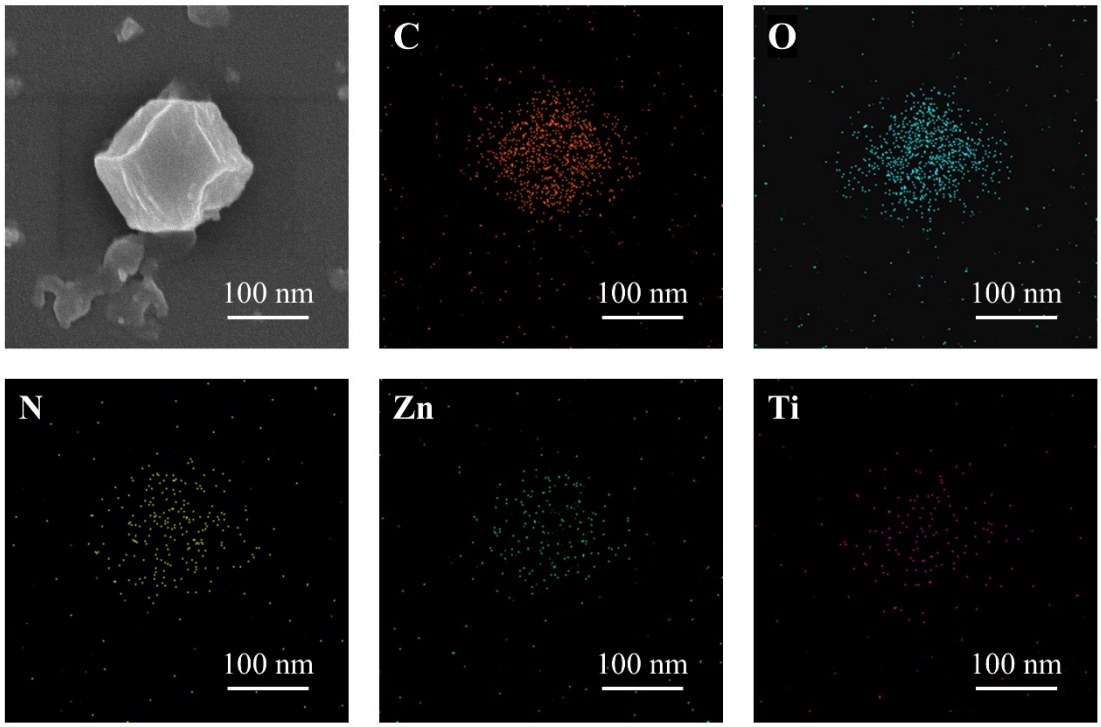

Fig. S3. EDS spectrum of PDT@ZIF-90.

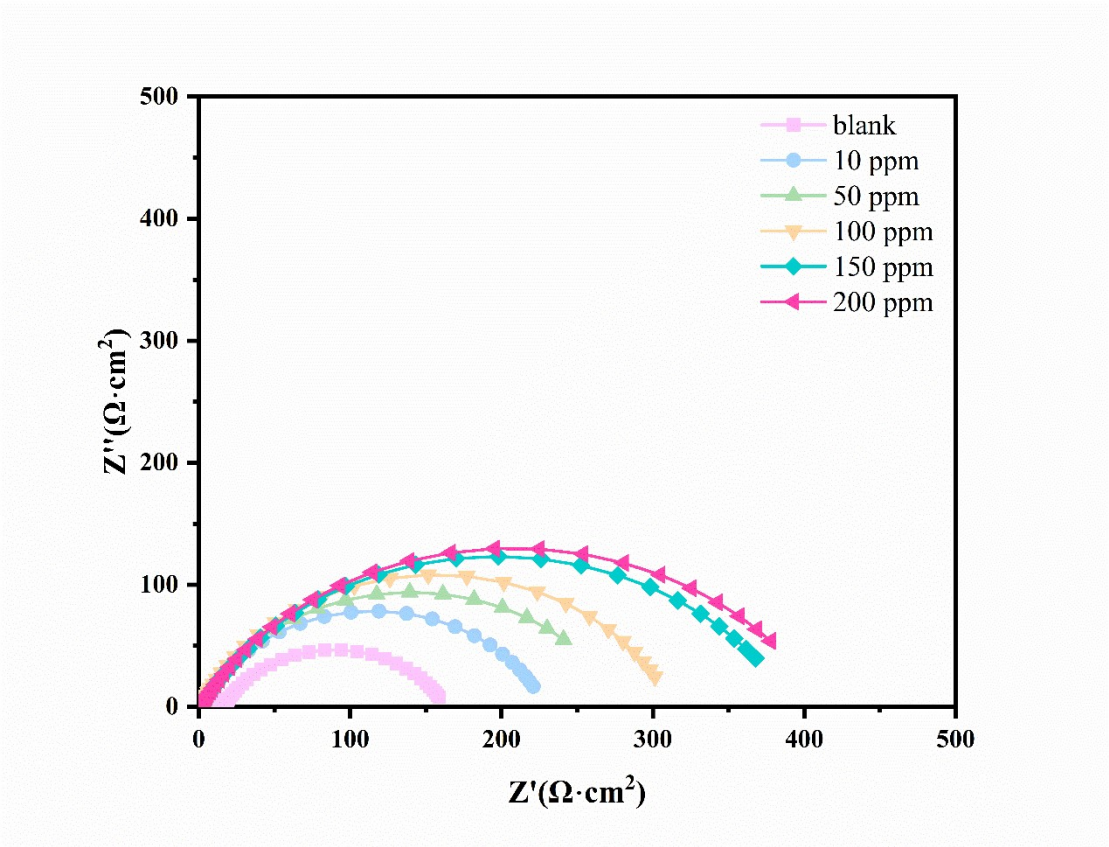

Fig. S4. Nyquist curves of different concentrations (10, 50, 100, 150 and 200 ppm) of ZIF-90 at 298 K for 72 h.